Vietnam Journal of Catalysis and Adsorption
Tạp chí xúc tác và hấp phụ Việt Nam

http://jca.edu.vn

Preparing the adsorption material from coconut trunk to remove As(V) in aqueous solution

Ho Sy Thang[1], Nguyen Thuy Kieu[1], Le Thi Thanh Xuan[1], Dang Kim Tai[1], Ly Huy Hoang[1], Nguyen Minh Thao[1,*], Tran Hoai Lam[2], Nguyen Thi Lan Huong[3], Bui Tho Thanh[4]

[1] *Dong Thap University, Cao Lanh 870000, DongThap province, Vietnam*
[2] *Ho Chi Minh City University of Industry and Trade, Ho Chi Minh City, Vietnam*
[3] *Ho Chi Minh City University of Natural Resources And Environment, Ho Chi Minh City, Vietnam*
[4] *University of Science, Vietnam National University Ho Chi Minh City, Vietnam*
** Email: nmthao@dthu.edu.vn*

ARTICLE INFO

Received: 11/11/2025
Accepted: 30/03/2026
Published: 30/03/2026

Keywords:
Adsorption; arsenic; coconut trunk

ABSTRACT

Coconut trunks were used as raw materials to manufacture As(V) adsorbent materials in aqueous solution. The biochar AC700 was prepared by heating coconut trunk biomass at 700 °C for 1 hour. The AC700 material was modified by 1.5 M H_3PO_4 solution to form the AC700/H_3PO_4 material. The material 's structure was characterized by X-ray diffraction, FT-IR, SEM, EDS, and the BET method. The specific surface area of AC700 and AC700/H_3PO_4 material are 448.136 $m^2.g^{-1}$ and 732.373 $m^2.g^{-1}$, respectively. The study on adsorption kinetic models and adsorption isotherms indicated that the As(V) adsorption process by AC700/H_3PO_4 followed the pseudo-first-order kinetic model and the Langmuir adsorption isotherm model. The prepared material can effectively remove the As(V) in aqueous solution. The density functional theory calculation simulated the hydrogen interaction between material and As(V), so material can absorb the As(V) in aqueous solution.

Introduction

Arsenic (As) is an inorganic pollutant in the groundwater that supplies people's consumption. The allowable concentration of Arsenic in water is 0.01 $mg.l^{-1}$ according to the World Health Organization (WHO) standards and QCVN 01: 2009/BYT compiled by Department of Preventive Medicine & Environment and promulgated by MOH's Minister at the Circular No.04/2009/TT-BYT dated 17th June 2009 of Vietnam Ministry of Health on the issuance of "National technical regulation on drinking water quality" [1,2]. Arsenic in the environment includes As(0), As(III), and As(V), which need to reduced because of our highly toxic.

Many methods can be used to remove As from water as ion exchange, chemical precipitation, membrance technologies... [3-6]. Biochar and the modified-biochar materials are the potential material to adsorb the organic and inorganic polutions [7-10]. In March 2026, an investigation on phosphoric acid-activated biochar from jacaranda fruits was prepared with high a Brunauer–Emmett–Teller (BET) surface area and enriched surface functionalities [10]. The phosphate bond bridge can change the structure and surface area of biochar, improving As(V) adsorption [10-12]. In this study, H_3PO_4 is used to modify biochar from coconut trunks to create an adsorption material for removing As(V) from aqueous solution.

Experimental

Chemical

Coconut trunk is a by-product that is taken from gardens in Cao Lanh ward, Dong Thap province. The

https://doi.org/10.62239/jca.2026.011

H_3PO_4 98% is purchased from Guangzhou Guanghua Sci-Tech Co (China). The standard arsenic As(V) 1000 ppm solution is purchased from Merck (Germany).

Methods

Coconut trunks taken from the garden in Cao Lanh ward, Dong Thap province, were washed, chopped, and dried to a constant mass at 105 °C. The dried material was pyrolysed in the oxygen limited condition at 700 °C for 1 hour in ceramic mug with lid, with a heating rate of 5 °C/min, to obtain biochar, which was then crushed into powder, and denoted as AC700. The process of transforming biochar with H_3PO_4 is as follows: 10 g AC700 is added to 140 mL of 1.5 M H_3PO_4 solution at 80 °C, with stirring at 400 rpm on a magnetic stirrer. Let the solution cool, then filter it out. The solid part is placed into a porcelain cup, covered, and heated at 500 °C for 2 hours [13]. After cooling to room temperature, wash with distilled water until the filtrate has a pH of 6-7, then dry, grind finely to obtain biochar transformed with H_3PO_4, denoted as AC700/H_3PO_4. The materials were characterized by X-ray diffraction, FT-IR, SEM, EDS, and the BET methods.

Study on the adsorption capacity of As(V) in water: 0.250 g of material was poured into an Erlenmeyer flask containing 100 mL of a 100 ppb As(V) solution, stirred at 400 rpm. The adsorption times were 2 hours, 5 hours, 10 hours, 24 hours, 30 hours, 34 hours, and 48 hours, respectively. The As(V) solution concentration was analyzed using the ICP-MS method. The adsorption capacity, adsorption kinetic model, and adsorption isotherm were evaluated.

To have more informations in the As(V) removing by adsorption into material, the simulation structure was built and optimized using density functional theory (DFT) [14,15] with PBE functional [16] and def2-TZVP basis set using ORCA 4.2.1 package [17,18].

Results and discussion

Material characteristics

The X-ray diffraction pattern of the material shows 2 theta signal range from 8 to 27°, characteristic of amorphous carbon. The peaks with vigorous intensity are characteristic of metal oxides in the coconut tree trunk. This result is consistent with the EDS analysis results (Figure 1c and Table 1). The analysis results show that the main components include 88.06% C, 8.04% O. Some elements have small proportions, such as Na (1.25%), Al (0.41%), P (0.22%), Cl (1.13%), K (0.38%), and Ca (0.20%). After modification, the characteristic peaks of oxides in the AC700 sample disappeared due to dissolution in acid. The peak position at 2theta ~25° has a strong intensity characteristic of the graphite carbon structure. The diffraction peak at 43° is characteristic of C(100), the diffraction peak at 54° is characteristic of C(004) [19,20]. In Figure 1d, the signals of Na, K, Ca, and Cl elements are not seen in EDS analysis because of dissolution. The peak at two keV indicates that the P element is incorporated into the biochar structure.

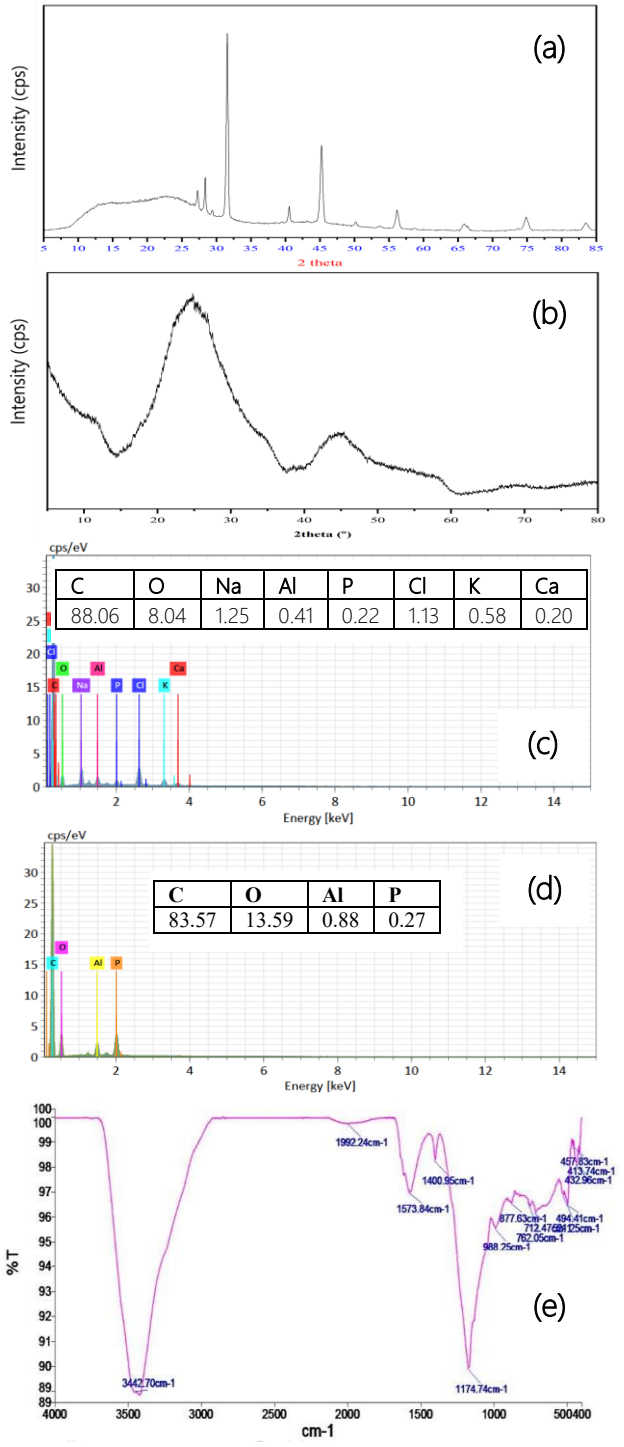

Fig. 1: Characterizations of AC700 and AC700/H_3PO_4. The XRD diagram of (a) AC700; (b) AC700/H_3PO_4. The EDS results of (c) AC700; (d) AC700/H3PO4. (e) The FT-IR spectroscopy of AC700/H_3PO_4

https://doi.org/10.62239/jca.2026.011

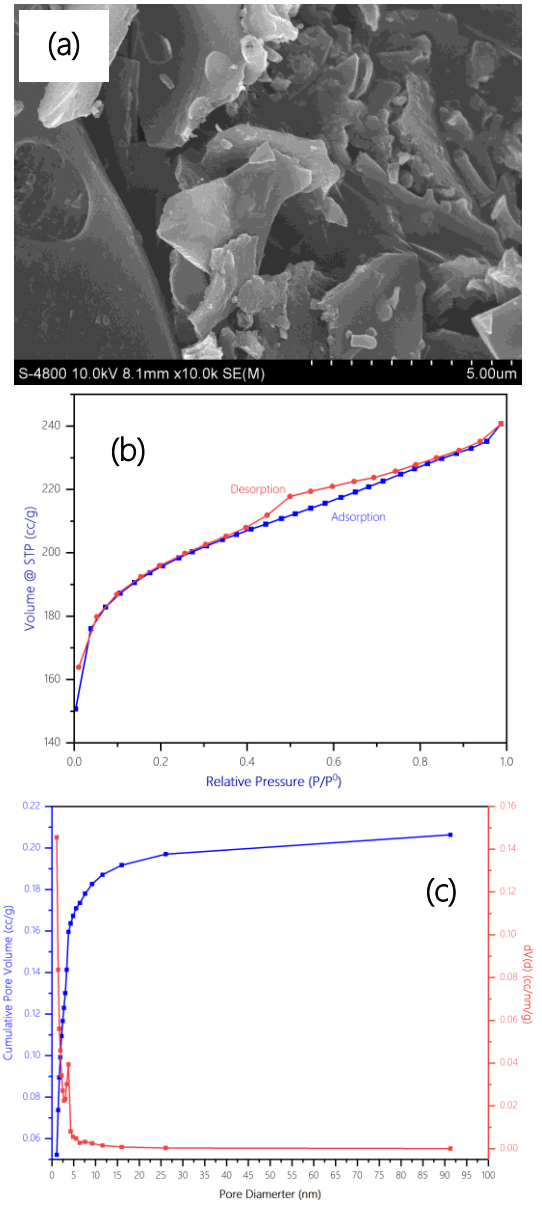

Fig. 2: The (a) SEM, (b) The nitrogen adsorption-desorption BET curves, and (c) BJH curves results of AC700/H_3PO_4.

The FT-IR vibrational spectrum of the AC700/H_3PO_4 material is shown in Figure 1e. The peak at 3442 cm^{-1} is characteristic of the O-H stretching vibration. The peak at 1573 cm^{-1} is characteristic of the C=C bond vibration of an aromatic ring or C=O vibration. The peak at 1400 cm^{-1} is characteristic of the C-H bond vibration. Peak at 1174 cm^{-1} is characteristic of valence vibrations of bonds in HO-P=O, polyphosphate, or phosphate chains. Peaks at 988 cm^{-1} can be attributed to polyphosphate chains (P-O-P) or acid-phosphate ester groups (P+-O-). The fingerprint range of 1100 - 850 cm^{-1} is vibrational characteristic of P-OH and polyphosphate. These peaks are attributed to the formation of cellulose phosphate esters through the heating of biochar with phosphoric acid [21,22];

SEM images in Figure 2a reveal that the obtained biochar has a rough surface with numerous patches of varying sizes and numerous gaps between the particles. The BET and BJH analysises show that the biochar obtained from calcining coconut tree trunks at 700°C has a specific surface area of 448.136 $m^2.g^{-1}$. The specific surface area of the biochar sample obtained when calcining coconut tree trunks at 500 °C is 3.582 $m^2.g^{-1}$ and calcined at 900 °C is 535.156 $m^2.g^{-1}$ [20]. When the biochar is modified with H_3PO_4 solution, the surface area of the obtained material increases to 732.373 $m^2.g^{-1}$ by BET method from nitrogen adsorption-desorption isotherm analysis shown in Fig 3b. We can also observed from the surface area in H_3PO_4-modified biochar derived from jacaranda fruits is 791 $m^2.g^{-1}$ [10]. We also observe in the report [23]. Figure 3c shows the correlation between the pore volume and pore diameter of the AC700/H_3PO_4 sample, in which the pore with a diameter of 1.17 nm has the pore volume of 0,206 $cc.g^{-1}$.

The adsorption of As(V)

To investigate the end time of the adsorption reaction, we experimented to monitor the change in the concentration of the pollutant in the solution over time at an initial concentration of C_0 = 100 ppb. The time periods investigated were 0, 2, 5, 10, 24, 30, 34, and 48 hours, respectively. The results showed that the pollutant concentration decreased rapidly in the first 10 hours, from 100 to 53.5 ppb, then decreased slowly and almost stabilized after approximately 30–34 hours, with an equilibrium concentration value of approximately 22.4 ppb. The graph shows that the adsorption time for the system to reach equilibrium was 30 hours. The above results show that the concentration of As(V) in the solution decreased sharply over the first 10 hours, from 100 to 53.5 ppb, corresponding to a rapid increase in adsorption capacity from 0 to 0.0186 $mg.g^{-1}$. This rapid decrease may be attributed to the presence of numerous vacant sites on the surface of the adsorbent material, enabling As(V) ions to access and bind easily. After 10 hours, the adsorption rate decreased significantly; the adsorption capacity only increased slightly from 0.0186 $mg.g^{-1}$ (10 hours) to 0.0305 $mg.g^{-1}$ (30 hours), and almost stabilized after 34–48 hours with a q_e value of ≈ 0.0310 $mg.g^{-1}$. Therefore, the chosen reaction time as 30 hours is appropriate to ensure that the system reaches complete equilibrium. Previous studies on adsorbents from biomass sources or surface-modified materials also reported equilibrium times ranging from 24 to 48 hours, depending on the pore structure and density of active sites of the material [24]. According to the study by Nand

https://doi.org/10.62239/jca.2026.011

et al. [4], the best As(V) removal efficiency was achieved using an iron-modified carbon material from deoiled Mentha waste after 24 hours at pH 7.5 with a material dosage of 25 mg/50 ml of solution.

Explainable interactions in Density Functional Theory

Biochar include aromatic carbon lactic and hemicellulose. The interactions between them and As(V) were calculated by density functional theory. The aromatic with hydroxyl functional structure (Ar-O-H) and phosphate modified structure (Ar-O-PO_4) are calculated to interact with As(V) as in Fig 3.

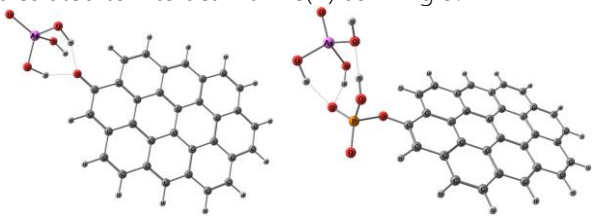

Fig. 3: Simulate the interaction between the aromatic carbon structure in biochar and As(V) by the DFT at the PBE/def2-TZVP level.

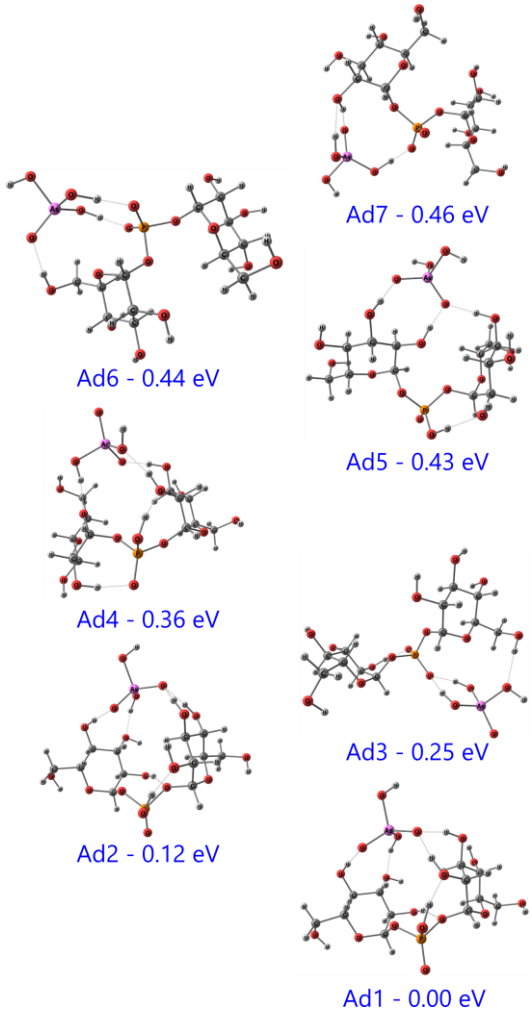

Fig. 4: Some interactions between hemicellulose - As(V) calculated by the DFT at PBE/def2-TZVP level

In Fig. 4, the structures with the minimum energy on the potential energy surface exhibit the presence of P as a bridge, which facilitates the movement of the monosaccharide closer together, thereby increasing the ability to form multiple hydrogen interactions with As(V). In addition, As(V) particles can also interact right at the phosphate position thanks to the formation of hydrogen bonds between O (phosphate) and H in As(V) and hydrogen bonds between OH groups attached to the C6 ring with As(V). The results indicate that the structures exhibit good interactions due to the formation of hydrogen bonds between O and H atoms in As(V) and the material's composition. Creating an acidic environment (pH~3) increases the ability to form hydrogen bonds.

Adsorption kinetic model study

The pseudo kinetic models are include [25]:

First-order: $\ln(q_e - q_t) = \ln(q_e) - k_1.t$

Second-order Type 1: $1/(q_e - q_t) = 1/q_e + k_{21}.t$

Second-order Type 2: $t/q_t = 1/(k_{22}.q_e^2) + t/q_e$

The research results as shown in Figure 5 showed that the first-order apparent kinetic model was suitable for describing the adsorption process of As(V) on materials made from coconut trunks, with an R^2 value of 0.99545. The obtained adsorption rate constant was k_1=0.125 h^{-1}, showing that the process took place relatively quickly in the first 10 hours, then gradually decreased and reached equilibrium after about 30 hours.

The adsorption kinetic model analysis results indicate that the adsorption process of As(V) on the investigated material is most consistent with the first-order apparent kinetic model, characterized by a high correlation coefficient value that is significantly larger than that of the second-order apparent kinetic model. This indicates that the adsorption rate primarily depends on the concentration of the remaining pollutant in the solution, consistent with the physical adsorption mechanism.

The results of the adsorption kinetic model analysis show that the adsorption process of As(V) on the investigated material is most consistent with the pseudo-first-order model model, with a high correlation coefficient value (R^2 = 0.99545), significantly larger than that of the pseudo-second-order Type 1 model (R^2 = 0.94841). This indicates that the adsorption rate primarily depends on the concentration of the remaining pollutant in the solution, consistent with the physical adsorption mechanism. The pseudo-second-order Type 2 model also showed a relatively high correlation R^2 = 0.99027, it was quitely lower than that of the first-order model, indicating that surace

https://doi.org/10.62239/jca.2026.011

interactions as hydrogen bonds influence the adsorption mechanism.

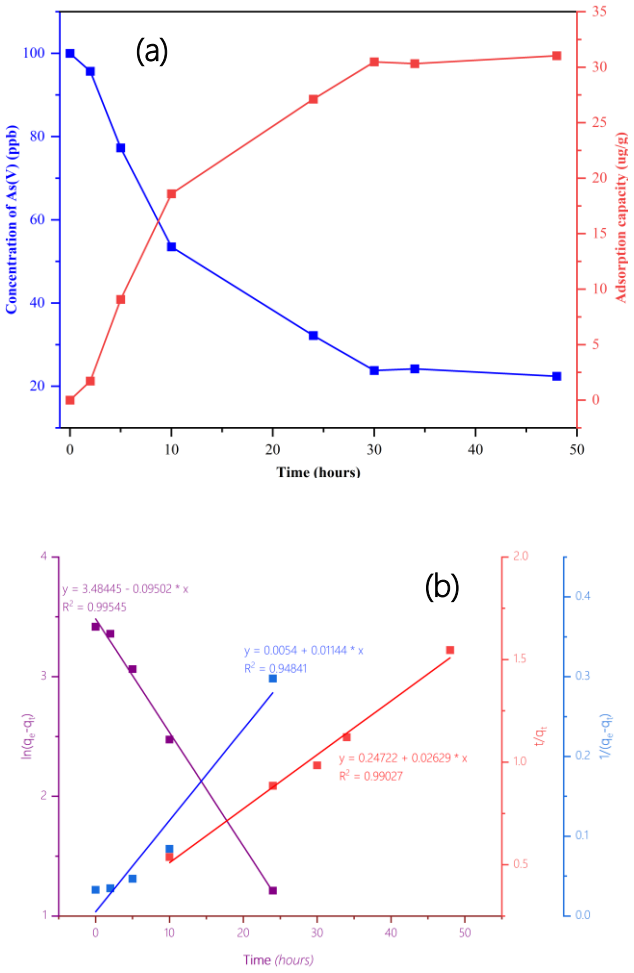

Fig. 5: The As(V) adsorption kinetic study (a) The concentration of As(V) and capacity adsorption in time. (b) Pseudo-first-order model (brown color line), Pseudo-second-order Type 1 model (blue color line) and Pseudo-second-order Type 2 model (red color line)

The adsorption rate coefficient value obtained from the pseudo-first-order model (k_1 = 0.125 h^{-1}) was higher than that of the pseudo-second-order Type 2 model (k_{22} = 0.01144 $g{\cdot}mg^{-1}.h^{-1}$), confirming that the adsorption rate was fast in the initial stage and reached equilibrium when the adsorption sites were gradually occupied. This result is consistent with many previous studies that describe the adsorption kinetics of As(V) using materials with developed capillary structures, in which the primary mechanism is physical adsorption [26,27]. Thus, the first-order apparent kinetic model is the most suitable to describe the adsorption process of As(V) on the studied material, and at the same time correctly reflects the dominant physical adsorption nature in the system.

Adsorption isotherms study

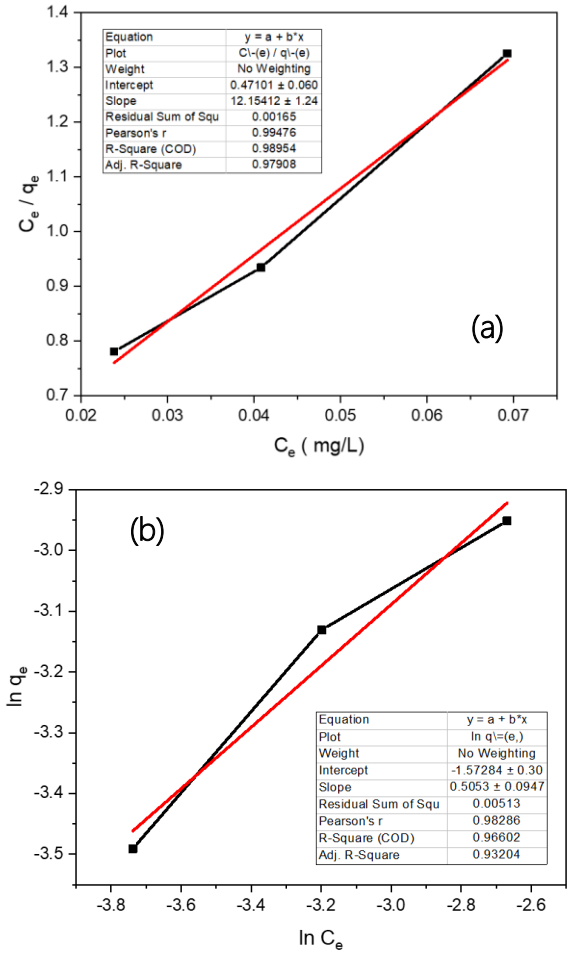

Fig. 6: The As(V) adsorption isotherm study (a) Langmuir and (b) Freundlich

The As(V) adsorption isotherm study showed that both the Langmuir and the Freundlich models described the adsorption process well, with the coefficients of determination R^2 of 0.98954 and 0.96602, respectively. The Langmuir model exhibited a higher correlation, reflecting the adsorption mechanism that occurs mainly in a monolayer form on the surface with relative homogeneity of the material. The maximum capacity q_m = 0.0823 $mg.g^{-1}$ and the constant K_L = 25.80 $L.mg^{-1}$ showed the adequate adsorption capacity of As(V). Meanwhile, the values of n = 1.98 and K_F = 0.208 from the Freundlich model showed that the adsorption process occurred favorably on the heterogeneous surface. Both models accurately described the As(V) adsorption process. However, the Langmuir model showed a higher correlation, suggesting a predominantly monolayer adsorption mechanism, consistent with the active material's surface properties and the As(V) adsorption behavior in solution.

https://doi.org/10.62239/jca.2026.011

Conclusion

The study has successfully fabricated adsorbent materials from coconut tree trunks. The material obtained from heating coconut tree trunks at 700 °C has a specific surface area of 448.136 $m^2.g^{-1}$. The phosphoric acid modified carbon material AC700/H_3PO_4 was prepared under the condition of heating coconut trunk at 700 °C, modified with H_3PO_4 solution at 1.5 M concentration and heated at 500 °C for 2 hours, the specific surface area increased to 732.373 $m^2.g^{-1}$, capable of handling As(V) well with a removal efficiency of about 80% for 100 ml of As(V) solution with initial concentration of 100 ppb, material's mass of 0.25 g.

The adsorption process of As(V) by AC700/H_3PO_4 was found to follow both the pseudo-first-order kinetic model and the pseudo-second-order Type 2 model ; the Langmuir adsorption isotherm model. Density functional theory calculations explained the interaction between the material and As(V). The results demonstrated the material's ability to form numerous hydrogen bonds with As(V), thereby enhancing the As(V) capture capacity of the prepared material.

Acknowledgments

This research is supported by the project B2025-SPD-01.

References

1. M.o. Health, Circular on the issuance of "National technical regulation on drinking water quality", (2009).
2. J. Singh, A. Kumar, A. Pathak, T. Palai, Water Air Soil Pollut., 234(5) (2023) 308. https://doi.org/10.1007/s11270-023-06308-6
3. M.X. Pham, T.N. Nguyen, V.T. Bui, T.H.N. Nguyen, M.T. Nguyen, N.P. Bui, T.N.N. Nguyen, T.P. Mai, V.H. Nguyen, L.H. Tran, J. Appl. Polym. Sci., 141(12) (2024) e54749. https://doi.org/10.1002/app.54749
4. S. Nand, S. Kumar, B. Pratap, D. Dubey, M. Naseem, A. Patel, S. Shukla, P.K. Srivastava, J. Clean. Prod., 482 (2024) 144247. https://doi.org/10.1016/j.jclepro.2024.144247
5. P.N.T. Ho, T.B. Nguyen, C.D. Dong, H.T.T. Ho, C.T. Phan, T.H.D. Lai, Case Stud. Chem. Environ. Eng., 10 (2024) 100907. https://doi.org/10.1016/j.cscee.2024.100907
6. A. Acharya, G. Jeppu, C.R. Girish, B. Prabhu, V.R. Murty, A.S. Martis, S. Ramesh, Heliyon, 10(11) (2024) e31967. https://doi.org/10.1016/j.heliyon.2024.e31967
7. H. Khurshid, M.R.U. Mustafa, U. Rashid, M.H. Isa, Y.C. Ho, M.M. Shah, Environ. Technol. Innov., 23 (2021) 101563. https://doi.org/10.1016/j.eti.2021.101563
8. T. Wen, J. Wang, S. Yu, Z. Chen, T. Hayat, X. Wang, ACS Sustainable Chem. Eng., 5(5) (2017) 4371-4380. https://doi.org/10.1021/acssuschemeng.7b00418
9. U. Khalil, M. Bilal Shakoor, S. Ali, M. Rizwan, M. Nasser Alyemeni, L. Wijaya, J. Saudi Chem. Soc., 24(11) (2020) 799-812. https://doi.org/10.1016/j.jscs.2020.07.001
10. K. Damer, I. Hamadneh, M. Abu-Dalo, A. Al-Dujiali, Adsorpt. Sci. Technol., 2024 (2024) 1430388. https://doi.org/10.1177/02636174261430388
11. V.K. Jaiswal, A.D. Gupta, R. Kushwaha, R. Kumar, K. Singh, H. Singh, D. Mohan, R.S. Singh, J. Mol. Struct., 1324 (2025) 140904. https://doi.org/10.1016/j.molstruc.2024.140904
12. Y.I.E. Aboulsoud, Environ. Dev. Sustainability, 27 (2024) 16451-16474. https://doi.org/10.1007/s10668-024-04598-2
13. N.A. Fathy, S.A. Sayed Ahmed, R.M.M. Abo El-enin, Environ. Res. Eng. Manag., 59(1) (2012) 20-30. https://doi.org/10.5755/j01.erem.59.1.961
14. M. Khnifira, W. Boumya, J. Atarki, M. Sadiq, M. Achak, A. Bouich, N. Barka, M. Abdennouri, J. Mol. Struct., 1310 (2024) 138247. https://doi.org/10.1016/j.molstruc.2024.138247
15. N. Elboughdiri, I. Lakikza, A. Boublia, S.I. Aouni, N. El Houda Hammoudi, J. Georgin, D.S.P. Franco, H. Ferkous, D. Ghernaout, Y. Benguerba, Process Saf. Environ. Prot., 186 (2024) 995-1010. https://doi.org/10.1016/j.psep.2024.03.093
16. J.P. Perdew, K. Burke, M. Ernzerhof, Phys. Rev. Lett., 77(18) (1996) 3865-3868. https://doi.org/10.1103/PhysRevLett.77.3865
17. F. Neese, WIREs Comput. Mol. Sci., 12(1) (2022) e1606. https://doi.org/10.1002/wcms.1606
18. F. Neese, WIREs Comput. Mol. Sci., 8(1) (2018) e1327. https://doi.org/10.1002/wcms.1327
19. M. Jiao, Y. Shi, M. Li, H. Zhang, S. Li, H. Deng, D. Xia, Environ. Pollut., 361 (2024) 124857. https://doi.org/10.1016/j.envpol.2024.124857
20. T.T.X. Lê, M.T. Nguyễn, P.T. Nguyễn, T.B. Lê, T.K.P. Phạm, Dong Thap Univ. J. Sci., 14(04S) (2025) 121-131. https://doi.org/10.52714/dthu.14.04S.2025.1569
21. S.D. Alexandratos, X. Zhu, Vib. Spectrosc., 95 (2018) 80-84. https://doi.org/10.1016/j.vibspec.2018.01.007
22. D. Higai, Z. Huang, E.W. Qian, Environ. Prog. Sustainable Energy, 40(1) (2021) e13509. https://doi.org/10.1002/ep.13509
23. K.-Q. Du, J.-F. Li, M.A. Farid, W.-H. Wang, G. Yang, Ind. Crops Prod., 226 (2025) 120649. https://doi.org/10.1016/j.indcrop.2025.120649
24. N.B. Singh, G. Nagpal, S. Agrawal, Rachna, Environ. Technol. Innov., 11 (2018) 187-240. https://doi.org/10.1016/j.eti.2018.05.006
25. T.B.T. Võ, H.N. Nguyễn, M.T. Nguyễn, S.T. Hồ, J. Anal. Sci. Phys. Biol., 29 (2023) 105-110. https://vjol.info.vn/TCPTHLS/article/view/88283/74950
26. Y.-S. Ho, G. McKay, Process Biochem., 34(5) (1999) 451-465. https://doi.org/10.1016/S0032-9592(98)00112-5
27. M.K. Purkait, A. Maiti, S. Dasgupta, S. De, J. Hazard. Mater., 145(1-2) (2007) 287-295. https://doi.org/10.1016/j.jhazmat.2006.11.021